Available online at www.sciencedirect.com
ScienceDirect
Sensors and Actuators B 130 (2008) 343–350
SENSORS AND ACTUATORS B CHEMICAL
www.elsevier.com/locate/snb

A study of partially irreversible characteristics in a TTF–TCNQ gas sensing system☆

Jung-Yu Liao[a], Kuo-Chuan Ho[a,b,*]

[a] *Department of Chemical Engineering, National Taiwan University, Taipei 10617, Taiwan*
[b] *Institute of Polymer Science and Engineering, National Taiwan University, Taipei 10617, Taiwan*

Available online 10 August 2007

Abstract

The irreversible gas sensing behavior is investigated for TTF–TCNQ complex in the presence of NO_2 or O_2. Reactions with the gas molecules are the main reason to cause the irreversibility, which has been reported and supported by analytical data. The totally irreversible behavior was noticed when a TTF–TCNQ thin film was brought in contact with NO_2 gas. As for O_2 gas, however, only partially irreversible phenomenon was observed. For a TTF–TCNQ thin film that interacts with NO_2 or O_2 gas, the degree of irreversibility is determined by the competition ratio of the desorption rate to that of the reaction rate. A theory based on the competition concept was proposed and a general expression for three possible behaviors (totally reversible, totally irreversible, and partially reversible cases) in a gas sensing system was obtained. The O_2 sensing data match the theoretical prediction when the reaction and the adsorption are limited at the surface.

Keywords: Competition theory; Desorption; Irreversibility; Nitrogen dioxide sensor; TTF–TCNQ complex

1. Introduction

Tetrathiafulvalene (TTF)–tetracyanoquinodimethane (TCNQ) complex is a highly conductive [1] organic material, and is found to be sensitive to several gas species, such as NO_2, O_2, CO_2, etc. [2] Its individual components, TTF and TCNQ molecules and their individual derivatives, were reported to be ambient gas sensitive as well. There have been several discussions about how these materials are affected by the gases that surround them [3–8].

It is conceived that the structure of TTF [3] has been changed in IR spectrum (805–835 and 1270–1420 cm^{-1}) during NO_x exposure. The TTF derivative thin film [4] have been reported as well to become radical cation when dipping in iodine vapor. Henrion et al. [5] also reported that redox reaction, color change, as well as resistivity change can be observed when TCNQ-derived LB films were exposed to iodine gas. Perez et al. [6] discovered the change of charge transfer band of TCNQ derivative films under NO_2 exposure. Hertler et al. [7] and Suchanski and Duyne [8] showed that TCNQ and $TCNQ^{2-}$ anion decomposed in the presence of NO_2 and O_2 gases.

Compare to the existing evidence for TTF, TCNQ and their individual derivatives, there are only limited information about the effect of ambient gases on the sensing properties of a TTF–TCNQ complex. For example, Jouve et al. [2] reported that a TTF–TCNQ complex containing a polymer film shows irreversibility in NO_2 detection and partial reversibility in O_2 and H_2O detections. Based on the possible reactive nature of TTF–TCNQ complex, our previous work [9] had focused only on the irreversible sensing and modeling for NO_2 detection. One of the objectives of this study is to find out the reaction mechanism for a TTF–TCNQ complex when exposing to NO_2 or O_2 gas. Another objective is to establish a general model (completely reversible, partially reversible for O_2, and totally irreversible for NO_2) for those sensing materials that might be reactive.

2. Experimental

TTF–TCNQ complex is obtained by dissolving both TTF (Fig. 1(a)) and TCNQ (Fig. 1(b)) powders (Aldrich, TTF:97%; TCNQ:98%) into acetonitrile to form a 1:1 molar ratio radical cation–radical anion pair complex, as a precipitate

☆ Manuscript No. TP20#356 presented at the 11th International Meeting on Chemical Sensors, Brescia, Italy, 16–19 July 2006.

* Corresponding author at: Department of Chemical Engineering, National Taiwan University, Taipei 10617, Taiwan. Fax: +886 2 2362 3040.
E-mail address: kcho@ntu.edu.tw (K.-C. Ho).

0925-4005/$ – see front matter © 2007 Published by Elsevier B.V.
doi:10.1016/j.snb.2007.08.010

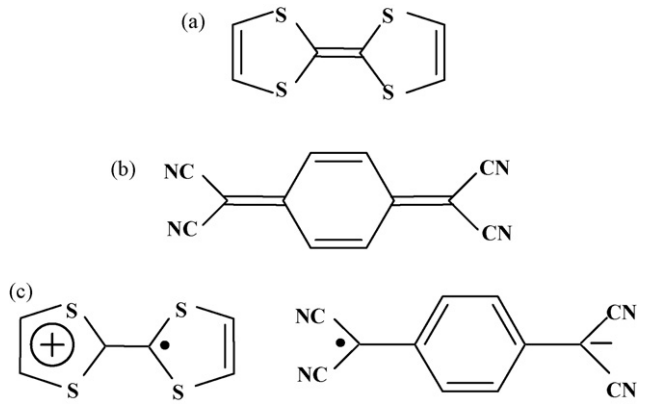

Fig. 1. The molecular structures of: (a) Tetrathiafulvalene, TTF; (b) Tetracyanoquinodimethane, TCNQ; (c) TTF–TCNQ complex.

(Fig. 1(c)). The preparation steps follow the procedure described in literature [1]. The complex powder is further purified by recrystallization in acetonitrile. Sensing thin film is thermally evaporated onto various substrates, including KBr (for FTIR), glass (for UV–vis, SEM and XRD), Pt coated quartz (for QCM), and Al_2O_3 with printed interdigitated gold electrode (for conductance) under 3×10^{-5} Torr vacuum. Film thicknesses are controlled at about 0.15–0.2 μm for both conductance and QCM measurements and 0.50–1.00 μm for other analytical experiments (XRD, UV–vis, FTIR and SEM). The deposition rate is *ca.* 5–10 Å/s.

The sensing film that face against the gas inlet at a flow rate of 200 ml/min is placed in a sensing chamber described elsewhere [9]. The sensing was carried out under room temperature. NO_2 and O_2 (from liquid air) gases are diluted with pure N_2 that is inert in this system. Unless stated otherwise, the standard sensing (exposure) process for analytical experiments was carried out for at least 12 h with 500 ppm NO_2 gas stream at 200 ml/min. The conductance was recorded by EG&G model 273A potentiostat/galvanostat. The QCM measurements were accomplished by Seiko EG&G QCA917, respectively. The UV–vis and FTIR spectra were carried out by Shimadzu UV-1601PC and Biorad FTS-40. The XRD and SEM data were obtained by Philips PW1710 (λ = 1.540 Å, scan rate = 3 deg/min) and Hitachi S-800, respectively. The detail experimental setup can be found in our previous work [9].

3. Results and discussions

3.1. Reaction involved sensing mechanism

In our previous work [9], a totally irreversible reaction is assumed in the model deduction. We are interested in finding the mechanism involving the conductive property and how the conductivity is affected. Several methods have been carried out to identify the possible reactions and conductive mechanisms.

3.1.1. Irreversible sensing response

Fig. 2(a) is a typical irreversible conductance response for NO_2 detection using a TTF–TCNQ complex. First of all, thin film was pretreated for 1 h under N_2 gas flow to ensure that moisture and other interfering impurities were totally removed. After approximately 43 h of 15 ppm NO_2 exposure, pure and inert N_2 gas was then purged again. However, it was found that the conductance does not recover when N_2 purging was in action. Instead of monitoring the transient of the conductance, a mass detection was also carried out. The thin film and gas flow conditions employed to obtain the data in Fig. 2(b) are identical to that in Fig. 2(a), the only difference is that a quartz crystal microbalance (QCM) was used to record the mass transient. Although several fluctuations was found in Fig. 2(b) during the entire NO_2 exposure process, one can notice an irreversible frequency decreasing (mass increase) trend which is consistent with the conductivity transient in Fig. 2(a).

After confirming the immobilization of NO_2, as judged by the increasing mass and decreasing conductance of a TTF–TCNQ complex, two reasonable possibilities may be drawn regarding the incoming NO_2 gas molecules, which are either "absorbed" within the film or "reacted" with the complex to form additional products and being immobilized inside the film.

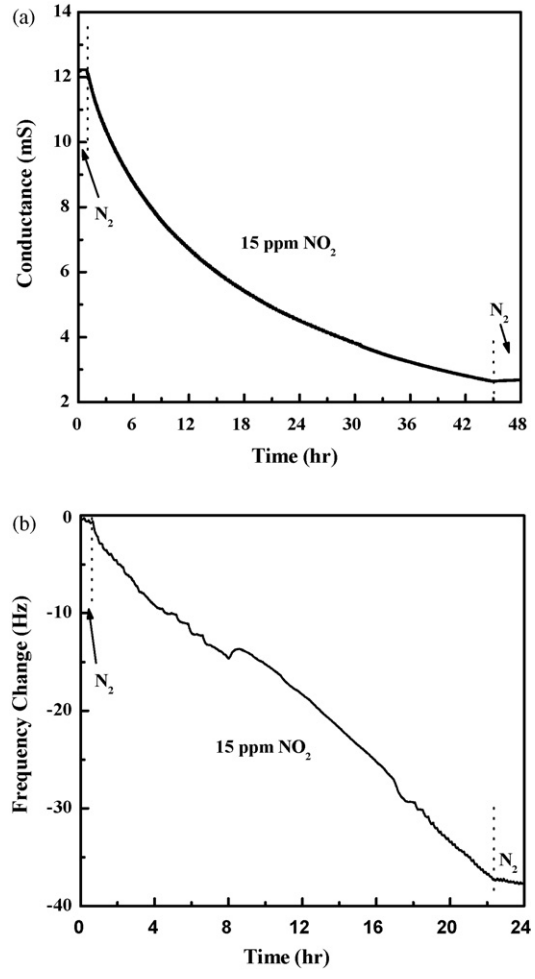

Fig. 2. Typical irreversible responses of NO_2 detection in (a) conductivity and (b) QCM frequency (mass) measurements.

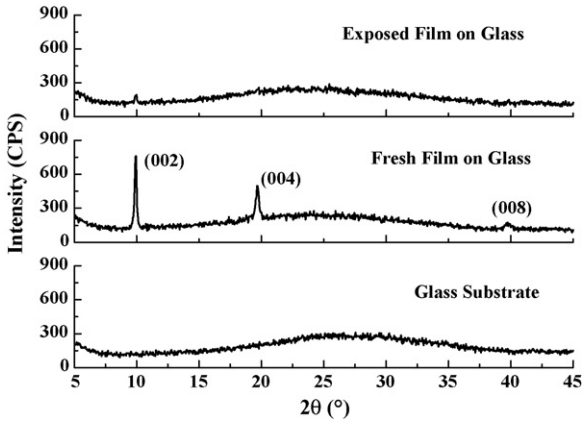

Fig. 3. XRD intensity for fresh and NO_2-exposed TTF–TCNQ thin films on glass substrate.

3.1.2. Crystal structure

The standard X-ray diffraction (XRD) pattern with three characteristic peaks [10] representing different packing planes is shown in Fig. 3. The crystalline intensity is dramatically decreased when the exposure process is finished. This suggested that the penetration of NO_2 molecules accompanied by reaction ruins the standard packing of this complex, hence lowering the intensity in the XRD pattern.

It is generally accepted that the distances between two parallel TTF and two parallel TCNQ molecules in the complex are about 3.47 and 3.17 Å [11], respectively. According to the kinetic theory of gas, the molecular diameter of a spherical molecule can be estimated by the viscosity of the gas [12]

$$d^2 = \frac{2.67 \times 10^{-20} \times (\mathrm{MT})^{1/2}}{\eta} \quad (1)$$

where, d is the diameter of spherical molecule, M the molar mass, T the temperature in Kelvin, and η is the viscosity of the gas. Assuming that all molecules are spherical molecules and that the viscosities for N_2, NO_2 and O_2 at 25 °C are 1.78×10^{-5}, 1.32×10^{-5} and 2.04×10^{-5} (pa s), respectively [13]. Thus, the diameters calculated from Eq. (1) for N_2, NO_2 and O_2 are 3.71, 4.87 and 3.58 Å, respectively, which are larger than the interplanar distance of TTF–TCNQ complex. It is highly unlikely that TTF–TCNQ complex itself will "absorb" the NO_2 molecule and allow the gas to diffuse into the interplanar space which is relatively narrower. Since the immobilization was observed in either conductance or QCM measurement (as seen in Fig. 2), it indicates that the immobilization of gas molecules will bring the destruction of the standard packing of the complex, as evidenced in Fig. 3. If a real stick type (O_2 and N_2) or curvy molecular (NO_2) shape is taken into account, the smoothly slip of molecules into the interplane becomes more difficult than a spherical one, and thus unlikely to happen.

3.1.3. Spectra analysis

Fig. 4(a) is the UV–vis spectra for a fresh and a NO_2-exposed film samples dissolved in acetonitrile. It can be found that three absorption peaks, which represent $TTF^{\bullet+}$ (318 nm, may has been shifted from 340 nm) and $TCNQ^{\bullet-}$ (743 and 838 nm, according

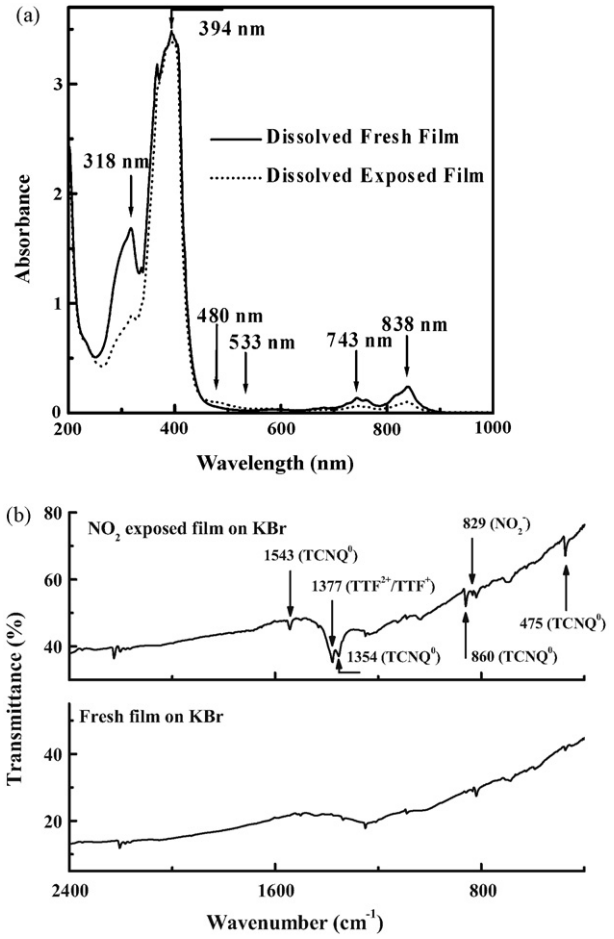

Fig. 4. (a) Visible spectra for dissolved fresh and NO_2-exposed TTF–TCNQ thin films; (b) IR spectrum for fresh and NO_2-exposed TTF–TCNQ thin films on KBr substrate.

to literatures [8,14–17], as summarized in Table 1) decrease after NO_2 exposure. The major peak at 394 nm, which is due to the oxidation of $TCNQ^{\bullet-}$ to form $TCNQ^0$ (both species absorb at 390–400 nm, referring to Table 1), still maintains its intensity after NO_2 exposure. Minor absorption at 533 nm represents the formation of TTF^{2+}.

It has been reported that $TCNQ^0$ molecule reacts with NO_2 to form terephthaloyl cyanide [7] and $TCNQ^{2-}$ ion reacts with O_2 to form $DCTC^-$ (α,α-dicyano-*p*-toluoyl-cyanide) ion [8]. Both reactions are basically similar and are mainly involved in a side chain transformation (two sides for NO_2 and one side for O_2). The difference is mainly determined by the oxidizing capability resulting from the active radical's existence in NO_2 molecule.

Table 1
The summarized UV–vis absorption peak ranges for TTF and TCNQ related species

Species	Peak ranges (nm)	References
$TCNQ^{\bullet-}$	400–455; 660; 728–760; 812–850	[14–16]
$TCNQ^0$	390–412; 430–432	[14–16]
$TTF^{\bullet+}$	340; 393–405; 435; 575; 653	[16,17]
TTF^{2+}	533	[16]
$DCTC^-$	480	[8]

Table 2
The summarized FTIR absorption peak ranges for TTF and TCNQ related species

Species	Peak ranges (cm^{-1})	References
$TCNQ^0$	3050; 2971; 2224; 1543; 1354; 1125; 1113; 862; 475	[18]
$TTF^{\bullet+}/TTF^{2+}$	805–835; 1270–1420	[3]
mixed	1300–1400	[19]
NO_2	1361; 1688; 770	[20]
NO_2^-	1325; 1270; 829	[20]

Therefore, it is believed that the minor peak at 480 nm in UV absorbance is due to the reaction with NO_2 gas forming $DCTC^-$ (Table 1).

The FTIR spectra for the fresh and the NO_2-exposed TTF–TCNQ thin films are shown in Fig. 4(b). The major absorption peaks (475, 860, 1354 and 1543 cm^{-1}, as summarized in Table 2) [18] found after NO_2 exposure represent the formation of $TCNQ^0$. Based on both UV and FTIR analyses, it is inferred that the major reaction involving $TCNQ^{\bullet-}$ is

$$NO_2 + TCNQ^{\bullet-} \leftrightarrow TCNQ^0 + NO_2^-, \quad \Delta G_2^0 \tag{2}$$

It is also reported that TTF^0 is oxidized when exposing to NO_2 with IR absorption region detected at 805–835 and 1270–1420 cm^{-1} [3]. It is possible that the peak at 1377 cm^{-1} is due to the oxidation of $TTF^{\bullet+}$, TTF^{2+} or their mixture [19]. Because the NO_2-exposed film is yellowish in appearance, not deep purple ($TTF^{\bullet+}$) [17], it is suggested that $TTF^{\bullet+}$ is further oxidized to yellowish di-cation (TTF^{2+}) in the actual reaction

$$NO_2 + TTF^{\bullet+} \leftrightarrow TTF^{2+} + NO_2^-, \quad \Delta G_3^0 \tag{3}$$

Since the bi-molecular exchanging from NO_2 to N_2O_4 are known to exist, the formation of NO_2^- (absorbance peaks at 1325, 1270, and 829 cm^{-1} [20]) is kinetically possible and thermodynamically feasible as described by the following reduction equation:

$$N_2O_4(=2NO_2) + 2e^- \leftrightarrow 2NO_2^-,$$
$$E_4^0 = 0.88\,V \text{ (versus NHE)} \tag{4}$$

In addition, the potentials for the redox couples TTF^{2+}/TTF^+ and $TCNQ^-/TCNQ^0$ are [21]

$$TCNQ^0 + e^- \leftrightarrow TCNQ^-,$$
$$E_5^0 = 0.13\,V \text{ (versus SCE) or } 0.37\,V \text{ (versus NHE)} \tag{5}$$

$$TTF^{2+} + e^- \leftrightarrow TTF^+,$$
$$E_6^0 = 0.66\,V \text{ (versus SCE) or } 0.90\,V \text{ (versus NHE)} \tag{6}$$

Therefore, the ΔG_2^0 for Eq. (2) is

$$\Delta G_2^0 = -1 \times F \times (E_4^0 - E_5^0) = -1 \times 96485 \times 0.51 = -49.2\,kJ/mol$$

and the ΔG_3^0 for Eq. (3) is

$$\Delta G_3^0 = -1 \times F \times (E_4^0 - E_6^0) = -1 \times 96485 \times -0.02 = 1.9\,kJ/mol \sim 0\,kJ/mol$$

Although ΔG_3^0 is a positive value, it should be taken to be a value close to zero. This is because the standard potentials of Eqs. (4) and (6) are too close (only 20 mV difference) when calculating the Gibbs free energy for Eq. (3). Therefore, Eq. (3) is taken as a reversible reaction which is possible to happen.

After completion of these reactions, the products become porous enough to be penetrated by the new incoming NO_2 molecules and the previous reactions repeat again. The remained porous product is called "tarnishing film [9]."

To summarize our previous discussion, a net reaction is proposed

$$2NO_2 + TTF - TCNQ \xrightarrow{k'} TTF^{2+} + TCNQ^0 + 2NO_2^- \tag{7}$$

This is to compare with the equation proposed in our previous work [9]

$$aNO_{2(g)} + TTF - TCNQ_{(s)} \xrightarrow{k'} [(NO_2)_a - (TTF - TCNQ)]_{(s)} \tag{8}$$

which can be denoted as

$$aB_{(g)} + A_{(s)} \xrightarrow{k'} AB_{a(s)} \tag{9}$$

where "a" is a stoichiometric factor between the reactants, which takes two NO_2 molecules to react with both $TTF^{\bullet+}$ and $TCNQ^{\bullet-}$, B represents NO_2, and A represents TTF–TCNQ complex, AB_a may be viewed as the comination of the mixed three products listed in Eq. (7).

3.1.4. Hypothetical mechanism

As far as we know, NO_2 does react with TTF–TCNQ complex, and it is reasonable to assume that the reaction is initiated by the strong interaction involving the unpaired electron (radical) located in the molecular orbital of NO_2 and the radical cation–radical anion pair of TTF–TCNQ complex (Fig. 1(c)). It is possible that the unpaired electron of NO_2 was attracted initially by the radical hopping through TTF–TCNQ complex packing. After the attracted NO_2 reacted with the complex, the conductive route is interrupted, as evidenced by both the continuous decrease in the conductance (Fig. 2(a)) and the increase in the mass (decrease in frequency, Fig. 2(b)) during NO_2 exposure. Based on the well-known structure of the TTF–TCNQ complex [11], which possesses 1-D (y-direction) an-isotropic conduction [22] and our previous discussion, we propose a hypothetical mechanism, as depicted in Fig. 5, to visualize the interaction. In this mechanism, the highly conductive property of the complex is contributed by the "active" hopping radical provided by the TTF–TCNQ complex. The un-paired, highly reactive NO_2 is attracted and reacted with the complex. The porous products are left behind (TTF^{2+}, $TCNQ^0$, NO_2^-, and small amount of

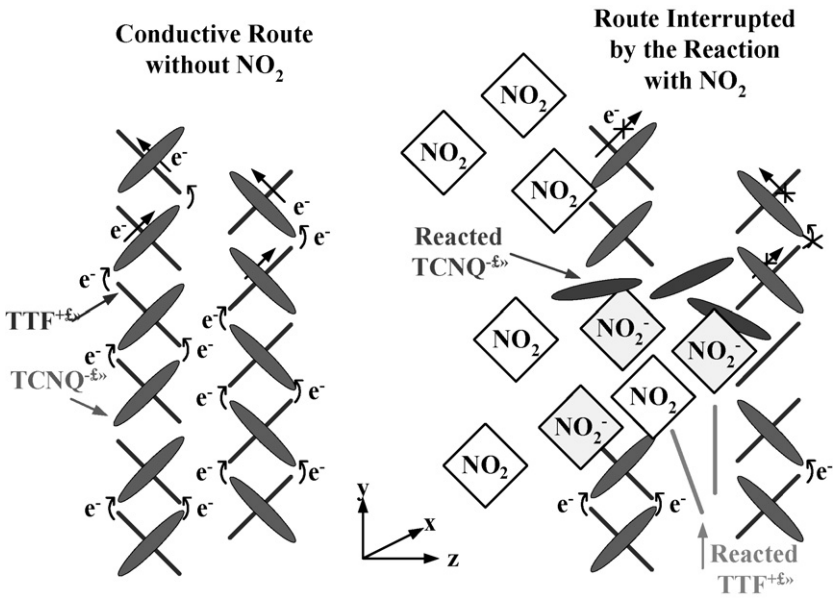

Fig. 5. Hypothetical conducting and reacting mechanism for the NO_2–TTF–TCNQ system.

DCTC$^-$) and the conduction route is destroyed, while the unreacted NO_2 keeps penetrating through the remains and react with the fresh complex.

3.1.5. Surface information from SEM

In the previous discussions, we imagine that the tarnishing film formed is a porous layer and allows larger molecules such as NO_2 to penetrate through. According to the SEM graphs shown in Fig. 6(a), which is the SEM image of a fresh TTF–TCNQ film coated onto a glass substrate, the surface of each chip of fresh TTF–TCNQ crystalline is quite smooth comparing to the NO_2-exposed film in Fig. 6(b). The increase in surface roughness after NO_2 exposure supports the formation of a porous tarnishing film.

3.2. General modeling of TTF–TCNQ-based sensors

The TTF–TCNQ complex not only is sensitive to NO_2 but also sensitive to O_2, as shown in Fig. 7. When exposing to O_2, the transient conductance shows partially irreversible sensing characteristics for the TTF–TCNQ complex. This sensing behavior is different from that of NO_2, as seen from Fig. 2(a). This means that the interaction between O_2 and TTF–TCNQ complex involves simultaneous adsorption/desorption and reaction processes.

In order to describe the partially irreversible behavior, the totally "irreversible reaction" model (proposed in our previous work [9]) and the totally "reversible adsorption/desorption [23]" model are adopted to form a general model.

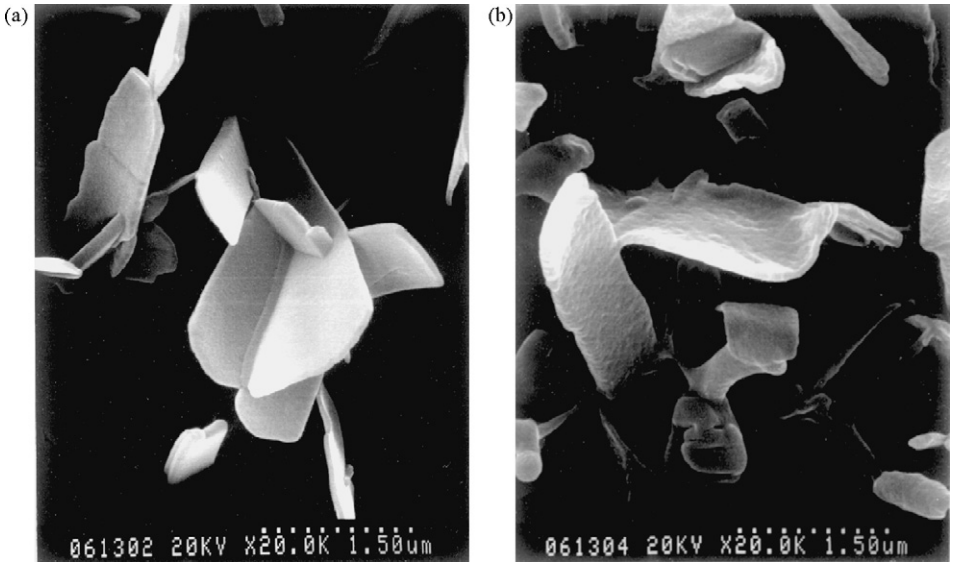

Fig. 6. SEM images for (a) fresh TTF–TCNQ and (b) NO_2-exposed TTF-TCNQ.

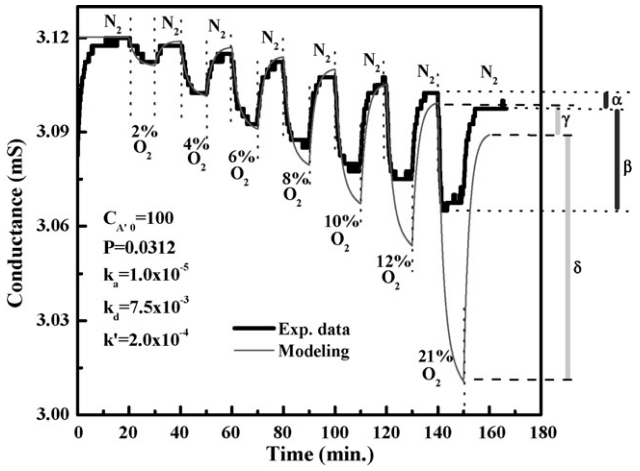

Fig. 7. Experimental data and modeling prediction for a partially irreversible response of O_2 sensing using a TTF–TCNQ complex. Segment α represents the actual reacted amount; β represents the actual adsorbed amount; γ is the predicted reacted amount predicted; and δ is adsorbed amount predicted.

The reversible adsorption/desorption theory is based on Langmuir isotherm, which has been reported to explain the sensing characteristic of NO_2 and a lead phthalocyaine thin film (PbPc) [23]. The general Langmuir expression is written as

$$aB_{(g)} + A(\text{thin film surface}) \underset{kd}{\overset{ka}{\longleftrightarrow}} A - B_a(\text{adsorbed}) \tag{10}$$

where "a" is the stoichiometric factor, B represents the incoming gas, A the sensing film which offers the surface area, and $A - B_a$ represents the adsorbed species.

Given the fact that O_2 is also reactive with the film, the adsorbed species ($A - B_a$) would react further with O_2 (since AB_a in Eq. (7) represents the final products), or

$$aB_{(g)} + A(\text{thin film surface}) \underset{k_d}{\overset{k_a}{\longleftrightarrow}} A$$

$$-B_a(\text{adsorbed}) \xrightarrow{k'} AB_a(\text{reacted}) \tag{11}$$

Several assumptions are made to validate the model before pursuing further analysis:

(i) Both adsorption/desorption and reaction are assumed to occur at the thin film surface only, which implies that the reacted amount and the rate of reaction are negligible. Once the reaction is taking place inside the film, this assumption is not valid.

(ii) In this work, "A" represents TTF–TCNQ, which is assumed to offer two ($TTF^{\bullet+}$ and $TCNQ^{\bullet-}$) "identical sites (denoted as A')" for the adsorption.

(iii) The reactive gas, B (e.g., O_2 or any other oxidizing gas), behaves similarly to NO_2 as seen in Eq. (7) with a stoichiometric factor of 2. Therefore, each site (A') adsorbs only one gas molecule. Therefore, the general model, Eq. (11), can be simplified as

$$B_{(g)} + A' \underset{k_d}{\overset{k_a}{\longleftrightarrow}} A' - B(\text{adsorbed}) \xrightarrow{k'} A'B(\text{reacted}) \tag{11′}$$

The actual reaction may be proposed as

$$2O_2 + \text{TTF} - \text{TCNQ} \xrightarrow{k'} \text{TTF}^{2+} + \text{TCNQ}^0 + 2O_2^-$$

where

$$O_2 + e^- \leftrightarrow O_2^-, \qquad E^0 = 0.56\,\text{V (versus NHE)}$$

The above reaction possesses less oxidizing capability than NO_2 does in Eq. (4), as judged by the values of E^0.

(iv) The conductance (G) measured is proportional to the fresh site concentration of A' ($C_{A'}$) which follows the reversible (semiconductor-type) kinetics concept (the adsorption of electron-drawing gases will localize the conducting radicals) [23], and

$$G = P \times C_{A'} \tag{12}$$

where P is a proportional constant.

(v) In order to quantify the partial irreversibility, the competition factor, f_C, is defined as

$$f_C = \frac{\text{desorption rate}}{\text{reaction rate}} = \frac{k_d C_{A-B_a}}{k' C_{A-B_a}} = \frac{k_d}{k'} \tag{13}$$

when $f_C \gg 1$ (or k_d is two orders higher than k', says $f_C > 100$, the reaction term can be neglected), Eq. (11) is simplified to a purely reversible adsorption/desorption case, such as Eq. (10); and when $f_C \ll 1$ (or k_d is two orders smaller than k', says $f_C < 0.01$, the desorption term can be neglected), Eq. (11) is then simplified to a pure reaction case, as depicted in Eq. (9), and $k_a = k'$ in this case.

When $0.01 < f_C < 100$, the desorption and reaction processes are in competition with each other. Both desorption and reaction cannot be ignored and should be taken into account. The rate expressions for Eq. (11′) are

$$\frac{dC_{A'-B}}{dt} = k_a C_{B0}(C_{A'0} - C_{A'-B} - C_{A'B}) - k_d C_{A'-B} - k' C_{A'-B} \tag{14}$$

$$\frac{dC_{A'-B}}{dt} = k' C_{A'-B} \tag{15}$$

where C_{B0} is the concentration of incoming gas B, which is a constant; $C_{A'0}$ the initial surface site concentration of fresh site A'; $C_{A'-B}$ is the surface concentration of adsorbed sites; $C_{A'B}$ is the surface concentration of reacted sites; $C_{A'}$ is the fresh site concentration ($=C_{A'0} - C_{A'-B} - C_{A'B}$); k_a, k_d, and k' are the adsorption, desorption, and reaction rate constants, respectively. The schematic expression for a competitive desorption/reaction model is shown in Fig. 8.

In order to solve Eqs. (14) and (15), two simplified forms are written as

$$C_1' = -EC_1 - FC_2 + I \tag{16}$$

$$C_2' = HC_1 \tag{17}$$

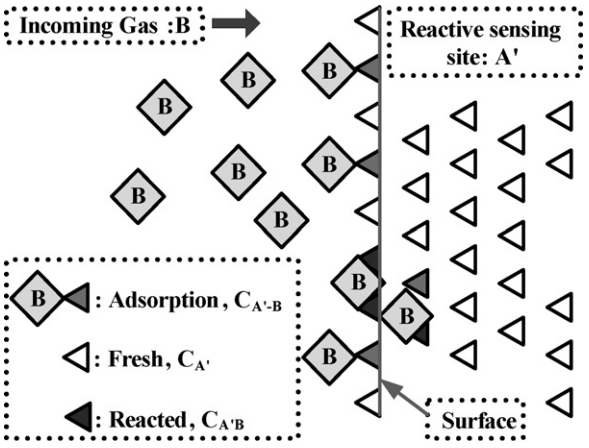

Fig. 8. The schematic representation for a competitive reaction/desorption model.

where $C_1 = C_{A'-B}$, $C_2 = C_{A'B}$, $E = (k_a C_{B0} + k_d + k')$, $F = k_a C_{B0}$, $I = k_a C_{B0} C_{A'0}$, $H = k'$, $C_{A'0}$ and C_{B0} are constants. By assuming the initial conditions as $C_1(t=0) = C_{10}$ and $C_2(t=0) = C_{20}$, Eqs. (16) and (17) are solved by the Laplace transformation, and the solutions can be classified into two cases:

(a) Adsorption process ($C_{B0} > 0$)

$$C_1 = C_{10}\, exp\left(-\frac{E}{2}t\right) \cosh\left(\sqrt{\frac{E^2}{4} - FH}t\right) + \frac{(I - FC_{20} - (EC_{10}/2))}{\sqrt{(E^2/4) - FH}} \exp\left(-\frac{E}{2}t\right) \times \sinh\left(\sqrt{\frac{E^2}{4} - FH}t\right) \quad (18)$$

$$C_2 = \frac{I}{F} + \left(C_{20} - \frac{I}{F}\right) \exp\left(-\frac{E}{2}t\right) \cosh\left(\sqrt{\frac{E^2}{4} - FH}t\right) + \frac{(C_{10}H + (C_{20}E/2) - (IE/2F))}{\sqrt{(E^2/4) - FH}} \exp\left(-\frac{E}{2}t\right) \times \sinh\left(\sqrt{\frac{E^2}{4} - FH}t\right) \quad (19)$$

(b) Desorption process ($C_{B0} = 0$)

Eqs. (18) and (19) can be further simplified when the desorption process starts by letting $I = 0 = F$, $I/F = C_{A'0}$, and $E = k_d + k'$ (because of $C_{B0} = 0$). One obtains

$$C_1 = C_{10} \exp[-(k_d + k')t] \quad (20)$$

$$C_2 = C_{20} + \frac{k' C_{10}}{k_d + k'}[1 - \exp[-(k_d + k')t]] \quad (21)$$

The totally reversible case is obtained by letting k' (or H) = 0, $C_2 = 0$, $C_{20} = 0$, $E = k_a C_{B0} + k_d$. Eqs. (18) and (20) can be reduced to

$$C_1 = \frac{I}{E} + \left(C_{10} - \frac{I}{E}\right) \exp(-Et) \quad (22)$$

$$C_1 = C_{10} \exp[-k_d t] \quad (23)$$

3.3. Results and data fitting

Both the experimental conductance transient and the fitted conductance transient, along with the fitted parameters, are shown in Fig. 7. Where $C_{A'0}$ is set to be 100 (real value is unknown); $P = 0.0312$, which is the proportional constant disscussed in Eq. (12). The obtained fitting parameters are: $k_a = 1.0 \times 10^{-5}$, $k_d = 7.5 \times 10^{-3}$, $k' = 2.0 \times 10^{-4}$, the competition factor, f_c, is 37.5, the range at which the competition of reaction and desorption does exist. It should be noticed that each adsorption/desorption step (every 10 min each step in Fig. 7) is fitted separately using the same set of k_a, k_d, and k'. That is, the value of C_1 ($C_{A'-B}$) and C_2 ($C_{A'B}$) at the end of one section are the "initial" values (C_{10} or C_{20}) for the next step. The values of C_1 and C_2 for the first step (2% O_2 adsorption) are set to be zero.

The model prediction fits the experimental data very well when operating under a lower concentration of O_2. The deviation begins to enlarge when the O_2 concentration is higher than 8%. Taking the final run (21% O_2) as an example, the actually reacted amount is represented by segement α in Fig. 7, however, the predicted value from the model is indicated by segement γ. On the other hand, the actually adsorbed amount is indicated by segement β, while the prediction from the model is segement δ. It can be found that the experimental amounts for both adsorpton and reaction are deviated from the model prediction at a higher O_2 concentration, especially noticeable for the adsorption process. It is possible that the numbers of adsorbing site are insufficient for further adsorption when exposed to a higher concentration of O_2. Smaller deviation is observed for the reaction process involves, and the actual amount of reaction is smaller than that of the predicted one ($\alpha < \gamma$), which can be explained by the modified tarnishing film model proposed in our previous work [9]. Since the reacted films are porous and the diffusion (or penetration) is dominant, as shown in Fig. 8, assumption (i) is no longer applied, thus explaining the deviation.

4. Conclusions

In this work, the irreversible behavior observed in NO_2 sensing with a vacuum evaporated TTF–TCNQ thin film is characterized and modelled. Both conductance and mass transients suggest the irreversibility has something to do with NO_2 immobilization. With the estimated diameters of gas molecules based on the kinetic theory of gas, the NO_2 most likely reacts with the complex before diffusing through the film is proposed. According to UV–vis and IR spectra data, as well as information from literatures, a net equation is proposed. In addition, XRD intensity, decreasing after NO_2 exposure, helps to explain the ongoing reaction that destroyed the crystal packing of the complex. Among all information available, we proposed a hypothetical

mechanism to realize the interaction between the NO_2 gas and the TTF–TCNQ complex. Coincident SEM surface images also support this mechanism.

Moreover, a general model which is suitable to explain three most common phenomena (reversible, partially irreversible, and totally irreversible) is proposed. The sensing of O_2 clearly follows the partially irreversible competition case with a competition factor, $f_C = 37.5$. The model fits the experimental data reasonably well at a lower O_2 concentration region, however, the deviation is noticeable at a higher O_2 concentration in which the thermal dynamic equilibrium and gas diffusion take place.

Acknowledgements

This work was sponsored by the National Research Council of the Republic of China (Taiwan) under grant numbers NSC 92-2214-E-002-037 and NSC 93-2214-E-002-020.

References

[1] J. Ferraris, D.O. Cowan, V. Walatka Jr., J.H. Perlstein, Electron transfer in a new highly conducting donor–acceptor complex, J. Am. Chem. Soc. 95 (1973) 948–949.
[2] C. Jouve, D. Jullien, B. Remaki, Conductive polyethylene as sensitive layer for gas detection, Sens. Actuators B 28 (1995) 75–80.
[3] R.J. Ewen, C.L. Honeybourne, European Patent, 0,490,572A1 (1992).
[4] S. Clemendot, M. Vandevyver, J.-P. Bourgoin, G. Derost, A. Ruaudel-Teixier, A. Barraud, Evaluation of conducting LB films based on ethylenedithiotetrathiafulvalene (EDT-TTF) derivatives for phosphine sensing, Sens. Actuators B 6 (1992) 197–201.
[5] L. Henrion, G. Derost, A. Ruaudel-Teixier, A. Barraud, Investigation of *n*-docosyl pyridinium, TCNQ Langmuir–Blodgett films as gas sensors, Sens. Actuators 14 (1988) 251–257.
[6] H. Perez, W. Budach, S. Palacin, G. Derost, A. Barraud, Nitrogen dioxide detection using low-conducting Langmuir–Blodgett films, Sens. Actuators B 26-27 (1995) 140–143.
[7] W.R. Hertler, H.D. Hartzler, D.S. Acker, R.E. Benson, Substituted quinodimethans. III. Displacement reactions of 7,7,8,8-tetracyanoquinodimethan, J. Am. Chem. Soc. 84 (1962) 3387–3393.
[8] M.R. Suchanski, R.P.V. Duyne, Resonance Raman spectroelectrochemistry. IV. The oxygen decay chemistry of the tetracyanoquinodimethane dianion, J. Am. Chem. Soc. 98 (1976) 250–252.
[9] K.C. Ho, J.Y. Liao, NO_2 gas sensing based on vacuum-deposited TTF–TCNQ thin films, Sens. Actuators B 93 (2003) 370–378.
[10] T.H. Chen, B.H. Schechtman, Preparation and properties of polycrystalline films of (TTF)(TCNQ), Thin Solid Films 30 (1975) 173–188.
[11] T.J. Kistenmacher, T.E. Phillips, D.O. Cowan, The crystal structure of the 1:1 radical cation-radical anion salt of 2, 2′-bis-1,3-dithiole (TTF) and 7,7,8,8-tetracyanoquinodimethane (TCNQ), Acta Cryst. B 30 (1974) 763–768.
[12] D.R. Lide, CRC Handbook of Chemistry and Physics, 81st ed., CRC Press, 2001, 6–46.
[13] T.E. Daubert, R.P. Danner, Physical and thermodynamic properties of pure chemicals, Hemisphere Publishing, New York, 1989.
[14] D.L. Jeanmaire, R.P.V. Duyne, Resonance Raman spectroelectrochemistry. 2. Scattering spectroscopy accompanying excitation of the lowest $^2B_{1u}$ excited state of the tetracyanoquinodimethane anion radical, J. Am. Chem. Soc. 98 (1976) 4029–4033.
[15] G. Inzelt, R.W. Day, J.F. Kinstle, J.Q. Chambers, Spectroelectrochemistry of tetracyanoquinodimethane modified electrodes, J. Electroanal. Chem. 161 (1984) 147–161.
[16] P.M.S. Monk, R.J. Mortimer, D.R. Rosseinsky, Electrochromism: Fundamentals and Applications, VCH, New York, 1995.
[17] F. Wudl, G.M. Smith, E.J. Hufnagel, bis-1,3-Dithiolium chloride: an unusually stable organic radical cation, J. Chem. Soc., Chem. Commun. (1970) 1453–1454.
[18] K.G.R. Pachler, F. Matlok, H.U. Gremlich, Merck FT-IR Atlas, VCH, Weinheim, 1988.
[19] S. Matsuzaki, N. Koga, I. Moriyama, IR spectra of solid state reaction products of TTF and iodine, Bull. Chem. Soc. Jpn. 56 (1983) 2090–2092.
[20] T. Hanawa, S. Kuwabata, H. Yoneyama, Gas sensitivity of polypyrrole films to NO_2, J. Chem. Soc., Faraday Trans. 1 (84) (1988) 1587–1592.
[21] C.D. Jaeger, A.J. Bard, Electrochemical behavior of donor-tetracyanoquinodimethane electrodes in aqueous media, J. Am. Chem. Soc. 102 (1980) 5435–5442.
[22] A. Figueras, J. Caro, J. Fraxedas, V. Laukhin, TTF–TCNQ thin films grown by organic CVD: texture and transport properties, Synthetic Met. 102 (1999) 1611–1612.
[23] C.J. Liu, J.C. Hsieh, Y.H. Ju, Response characteristics of lead phthalocyanine gas sensor: effect of operating temperature and postdeposition annealing, J. Vac. Sci. Technol. A 14 (3) (1996) 753–756.

Biographies

Jung-Yu Liao received his BS and PhD degrees in chemical engineering from National Taiwan University, Taipei, Taiwan, in 1999 and 2004, respectively. His research interest surrounds thin film process in general and gas sensors in particular. Currently, he is a researcher working on organic light emitting diodes (OLED) at the Material and Chemical Research Laboratories, Industrial Technology Research Institute (ITRI), Chutung, Hsinchu, Taiwan.

Kuo-Chuan Ho received BS and MS degrees in chemical engineering from National Cheng Kung University, Tainan, Taiwan, in 1978 and 1980, respectively. In 1986, he received the PhD degree in chemical engineering at the University of Rochester. The same year he joined PPG Industries, Inc., first as a senior research engineer and then, from 1990 until 1993, as a research project engineer. He has worked on the electrochemical properties of various electrode materials. He has applied surface science/interfacial engineering and electrochemistry/electrochemical engineering principles for improving the performances of electrochemical devices, including electrochemical sensors, electrochromic devices, and dye-sensitized solar cells, with emphasis on improving their electrochemical, at-rest, and thermal stabilities. Following a 6-year industrial career at PPG Industries, Inc., he joined his alma mater at National Cheng Kung University in 1993 as an Associate Professor in the Chemical Engineering Department. In 1994, he moved to the Department of Chemical Engineering at National Taiwan University. Currently, he is a Professor jointly appointed by the Department of Chemical Engineering and Institute of Polymer Science and Engineering at National Taiwan University.